JOURNAL OF MATERIALS SCIENCE **36** (2001) 1451–1457

# Mechanical properties of Fe-Co soft magnets

L. REN*, S. BASU‡, R.-HAI YU‡, J. Q. XIAO‡, A. PARVIZI-MAJIDI*
**Mechanical Engineering and ‡Physics and Astronomy, University of Delaware, Newark, Delaware 19716, USA*
*E-mail: info@me.udel.edu*

The tensile behavior of two magnetically soft alloys, Fe-49Co-2V and Fe-27Co, has been characterized as a function of testing temperature, grain size, and degree of long-range order. Several trends in the yield strength of the two alloys have been noted and possible mechanisms for their occurrence discussed. Ordering is found to markedly lower the yield strength of the Fe-49Co-2V. Both alloys exhibit three distinct regions in their yield strength vs. temperature curves. At lower and higher temperatures, i.e. regions I and III, the yield strength shows the normal drop with increasing temperature. In the intermediate temperature range (region II), however, Fe-49Co-2V with a B2 ordered structure demonstrates an anomalous strengthening with increasing temperature while the yield strength remains constant in the disordered Fe-27Co. Both alloys exhibit a Hall-Petch type relationship in their yield strength as a function of grain size and show a decrease in the strain hardening coefficient with increasing grain size. 

## 1. Introduction

Magnetically soft materials are used extensively in applications where low hysteresis loss, low eddy-current loss, high electric permeability, and high magnetic saturation induction are required. The study of such materials, however, has usually focused primarily on their magnetic function and they have seldom been systematically studied for their mechanical properties. This is because until recently these magnets were not used under demanding thermal and mechanical conditions. With recent technological advances and the expected use of magnets in expanding applications, such as the next generation high-speed aircraft, these materials must meet more stringent requirements of load and temperature. Therefore, current efforts in magnetic materials development are towards improving the mechanical properties and temperature capabilities.

In this paper, the room- and high-temperature mechanical properties of one class of soft magnetic materials, the iron-cobalt alloys ($Co_xFe_{1-x}$), were investigated. There is a renewed interest in these alloys because of their better high-temperature magnetic properties compared to other existing soft magnets, which makes them potential candidates for high temperature applications up to 600°C. Presently, the primary limitation of these alloys is not their high-temperature magnetic capability, but their mechanical properties, particularly creep resistance and fracture toughness. There have been a few studies on the mechanical properties of $Co_xFe_{1-x}$ alloys, particularly by Stoloff and co-workers [1, 2] as well as Chen [3] in the sixties, Rawlings and coworkers [4, 5] in the seventies and eighties, and Baker and coworkers [6, 7] in the last several years. Chen [3] investigated the connection between the brittleness of Fe-Co alloys and their degree of ordering and believed that the cause of brittleness in these alloys was partly their susceptibility to cleavage fracture, and not solely the long-range order. Koylu *et al.* [4] studied the relationship between long range order and low temperature deformation of the Fe-47Co-2V alloy using activation analysis. Pitt and Rawlings [5] reported that the microstructural features dominating the ductility of Fe-Co-2V and Fe-Co-V-Ni alloys are grain or sub-grain size, not the domain size of the ordered structure. When grain size was increased, the ductility decreased. However, despite these efforts, much work still remains to be done in understanding the structure-mechanical behavior relationships, developing mechanical property data bases for design, and improving some of the room- and high-temperature mechanical properties of these alloys.

In this paper, the mechanical properties of two widely used compositions of the Fe-Co alloy system, namely Fe-49Co-2V and Fe-27Co, were studied. Previous studies have indicated that the Fe-49Co-2V alloy has the best magnetic performance in the Fe-Co family of soft magnets, however, despite the addition of vanadium to increase ductility [8], it is still brittle. Also, the yield strength is not high enough for some of the more demanding applications. On the other hand, the ductility and toughness are better in Fe-27Co alloy but with trade-offs in magnetic performance and creep strength, which could be attributed to its disordered structure.

## 2. Experimental procedures

### 2.1. Materials and heat treatments

The Fe-Co alloys studied were Fe-49Co-2V and Fe-27Co manufactured by Carpenter Co., PA, and designated Hiperco 50 and Hiperco 27HS, respectively.

TABLE I The compositions of Fe-49Co-2V and Fe-27Co alloys

| | C | Mn | Si | Ni | Cr | Nb | V | Co | Fe |
|---|---|---|---|---|---|---|---|---|---|
| Fe-49Co-2V | 0.01 | 0.05 | 0.05 | — | — | 0.05 | 1.90 | 48.75 | Balance |
| Fe-27Co | 0.23 | 0.25 | 0.25 | 0.60 | 0.60 | — | — | 27.00 | Balance |

The compositions of the two alloys are given in Table I. The materials were supplied in the form of sheets with a thickness of 0.014 inch for Fe-49Co-2V and 0.01 inch for Fe-27Co. Parallel-sided tensile coupons, 0.5 in. × 8 in. with a 6 in. gage length, were cut from the sheets and given appropriate heat treatment for the investigation of the effects of temperature, degree of order, and grain size on the mechanical properties.

The temperature dependence of the mechanical properties was investigated for both Fe-49Co-2V and Fe-27Co alloys. For this, all the test coupons were given a baseline heat treatment of 2 hours at 800 °C in an argon environment, followed by cooling to room temperature at a rate of 90 °C/hour.

To assess the effect of ordering on the tensile behavior, test coupons of Fe-49Co-2V alloy were annealed for 2 hours at 820 °C in an argon environment and then cooled to room temperature at cooling rates of 30 °C/hr, 60 °C/hr, 90 °C/hr, air cooling, and brine quenching. This alloy undergoes an order/disorder transformation around 730°C. Although the selected cooling rates did not generate a range of the degree of long-range order, they produced largely disordered structures in air-cooled and brine-quenched samples and largely ordered structures for the three slower cooling rates, thus enabling a comparison of the mechanical properties of the ordered and disordered states.

Finally, in order to obtain a range of grain sizes for the investigation of the effect of grain size on the mechanical properties, test samples of both Fe-49Co-2V and Fe-27Co were first annealed at 820 °C for 10 min, 30 min, 60 min, 2 hr, 5 hr, and 20 hr, respectively, and then cooled to room temperature at a rate of 90 °C/hr.

### 2.2. Testing procedures

All the tension tests were conducted on an Instron Model 4484 testing machine. For room temperature testing, specimens were initially end-tabbed using glass/epoxy composite. However, end-tabbing was later abandoned as no significant difference was observed between the results obtained with tabbed and untabbed specimens. The majority of the specimens failed within the gauge section away from the grips. All the specimens tested at room temperature were instrumented with an electrical resistance strain gauge, Model EP-08-1254AC-350 from Micro Measurements Inc., for the recording of strain.

In order to study the temperature dependence of the mechanical properties, heat treated specimens of Fe-49Co-2V and Fe-27Co were tested in tension from room temperature (∼22 °C) to 800 °C at temperature intervals of 100 °C. Two samples were tested at each temperature. The high temperature tests were conducted in air using a series 3210 split furnace and a series XT16 temperature controller manufactured by Applied Test Systems, Inc. The furnace was equipped with K-type thermocouples for the temperature studied and was less than 4 in. long, thus only heating the test section of tensile coupons and leaving the grips cold.

To better analyze the effect of the temperature on the yield strength of the alloys, tensile tests were conducted at two crosshead speeds: a high speed of 0.3 in/min (0.127 mm/sec) for both alloys and a lower speed of 0.05 in/min (0.0212 mm/sec) for the Fe-49Co-2V alloy and 0.03 in/min (0.0127 mm/sec) for the Fe-27Co alloy. The crosshead speeds of 0.3 in/min, 0.05 in/min and 0.03 in/min correspond to strain rates of $8.3 \times 10^{-4}$/s, $1.39 \times 10^{-4}$/s and $8.3 \times 10^{-5}$/s, respectively. The slightly different lower strain rates for the two alloys were chosen somewhat arbitrarily.

For the effects of grain size and order/disorder, appropriately heat treated test coupons were tensile tested at room temperature and the full range of the stress-strain behavior was recorded. For these studies, three specimens were tested at each testing condition.

Following tensile failure, the fracture surfaces of all specimens were examined by scanning electron microscopy using a Phillips 504 scanning electron microscope in order to determine the failure mechanism.

## 3. Results and discussion

### 3.1. Temperature-dependence of the tensile properties

The effect of temperature on the tensile stress-displacement behavior of Fe-27Co alloy is shown in Figs 1 and 2 for the extension rates of 0.05 in/min and

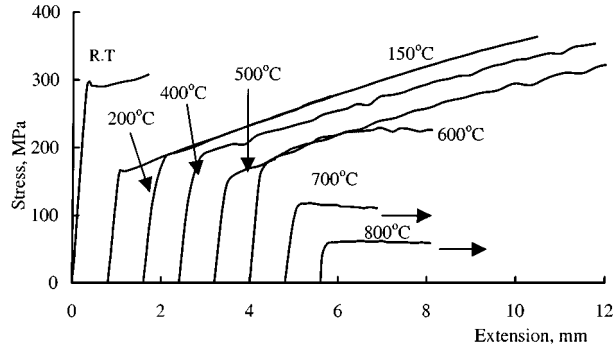


*Figure 1* Tensile stress-strain curves of Fe-27Co alloy as a function of temperature obtained at a rate of 0.03 in/min.

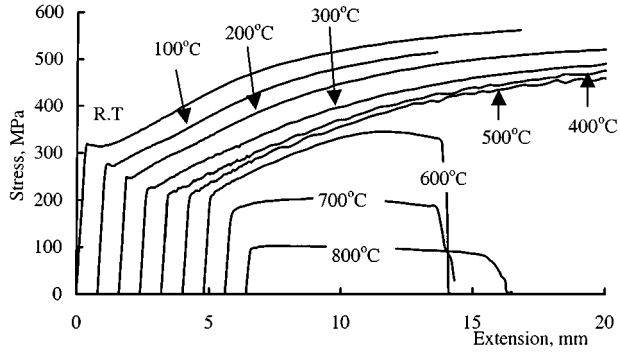


*Figure 2* Tensile stress-strain curves of Fe-27Co alloy as a function of temperature obtained at a rate of 0.3 in/min.

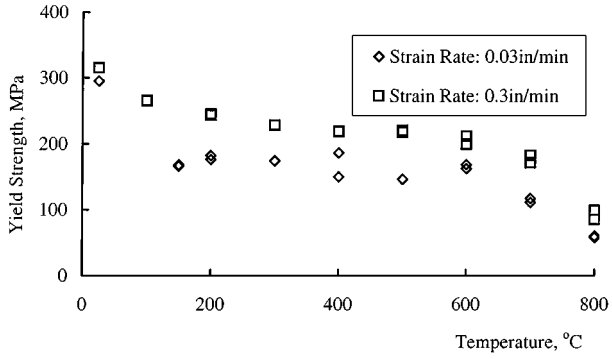


*Figure 3* The effect of temperature and strain rate on the yield strength of Fe-27Co alloy.

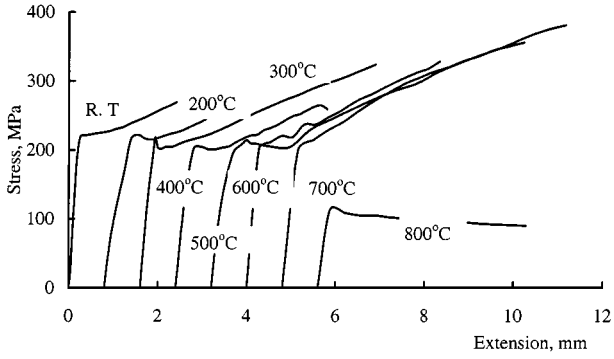


*Figure 4* Tensile stress-strain curves of Fe-49Co-2V alloy as a function of temperature obtained at a rate of 0.05 in/min.

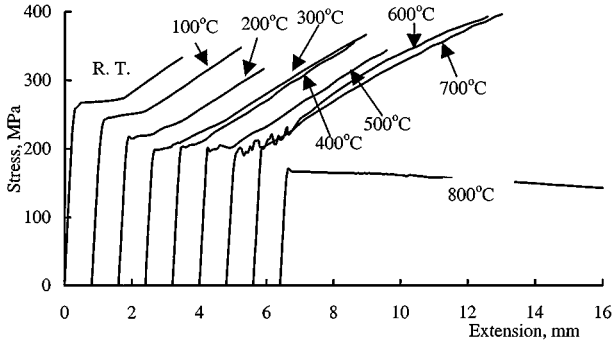


*Figure 5* Tensile stress-strain curves of Fe-49Co-2V alloy as a function of temperature obtained at a rate of 0.3 in/min.

0.3 in/min, respectively. Fig. 3 shows the yield strength as a function of temperature at both extension rates. The corresponding results for Fe-49Co-2V alloy are presented in Figs 4 to 6, respectively.

From Fig. 1, it is seen that Fe-27Co exhibits an upper yield strength followed by a small region of discontinuous yield at room temperature. The upper yield strength gradually disappears and the transition from elastic to plastic deformation becomes smooth as the temperature is raised above 200–300 °C. The yield strength drops significantly at temperatures beyond 600 °C as the material undergoes creep deformation.

The upper yield point and the discontinuous yield phenomenon are observed over a much wider temperature range, almost up to 600 °C, at the higher extension rate of 0.3 in/min (Fig. 2). Again, the strain begins to drop significantly beyond 600 °C. Specimens tested at 700 °C and 800 °C exhibited necking prior to final failure.

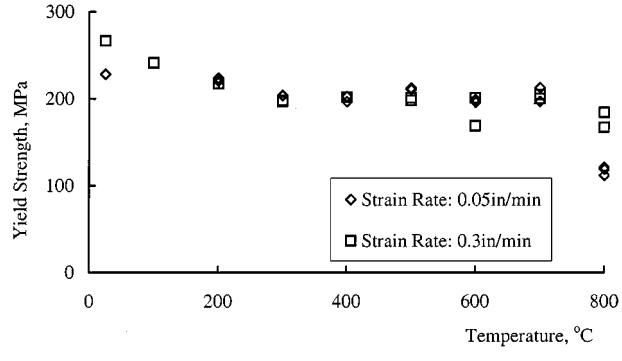


*Figure 6* The effect of temperature and strain rate on the yield strength of Fe-49Co-2V alloy.

As seen in Figs 4 and 5, the Fe-49Co-2V alloy displays a much longer discontinuous yield phenomenon than Fe-27Co alloy. The yield phenomenon continues up to a temperature of about 600 °C for both strain rates. In this case, the strain does not show a drop until a higher temperature of 800 °C. Specimens tested at the higher extension rate of 0.3 in/min exhibited necking at 800 °C.

The yield strength vs. temperature of Fe-27Co shows three distinct regions (Fig. 3). Region I extends from room temperature to about 200 °C, Region II from about 200 °C to about 600 °C, and region III from 600 °C. The yield strength falls in region I, then exhibits a plateau in region II, and finally falls again in region III. The data show similar trends for both strain rates. However, the magnitude of the strength is generally lower at the lower strain rate as would be expected. The Fe-49Co-2V alloy also shows a three-region behavior in its yield strength vs. temperature as shown in Fig. 6, except that in this case rather than a plateau region, the yield strength appears to actually slightly increase with increasing temperature in region II. In this alloy, region I is from room temperature to about 300 °C, region II from 300 °C to about 700 °C and region III from about 700 °C. A peak in the yield strength occurs around 700 °C, i.e., at about 0.5–0.55 $T_m$. Fig. 6 also shows that while the yield strength is higher at the higher strain rate in regions I and III, it is virtually insensitive to the strain rate in region II. The strain rate sensitivity of the strength in Region II is further discussed below.

Such a yield strength anomaly, in which the yield strength shows a positive temperature dependence, has long been known for some bcc-based intermetallic compounds such as $\beta$-CuZn and $D0_3$ $Fe_3Al$ [9–12]. Several researchers have since reported similar anomaly in other intermetallic compounds such as $L1_2$ $Al_3Ti$ and $L1_0$ TiAl and offered various explanations for its occurrence [13].

At temperatures below 725 °C, the Fe-49Co-2V alloy has a B2 ordered structure. Among the ordered intermetallics with a B2 structure similar to FeCo, FeAl is the most extensively studies [14–18]. Closely resembling the behavior of FeCo, FeAl also demonstrates anomalous strengthening at intermediate temperatures and a yield strength peak at around 0.4–0.5 $T_m$. Several models have been proposed for the yield strength anomaly in FeAl. Xiao and Baker [15] first

noted that the yield strength peak occurred at about the temperature of the transition from glide by APB-coupled $a/2\langle 111\rangle$ dislocations at low temperature to $\langle 100\rangle$ slip at high temperature. Baker and George [17] later suggested that this mechanism alone cannot explain the peak in the yield strength and offered a vacancy hardening model similar to that proposed by Morris [16]. Morris [16] identified the local climb of the APB-coupled dislocation partials as the cause of the anomaly. In his model, vacancy diffusion between the cores of the partials causes one partial to climb up and the other to climb down. Pinning points are thus generated in dislocation segments. The yield strength increases as the density of climb-dissociated partials rises with increasing temperature. In their vacancy hardening model, Baker and George [17] considered a pair of $a/2\langle 111\rangle$ dislocations that is gliding along a (110) plane separated by an APB. The second dislocation restores the disorder caused by the first dislocation within the APB. If a vacancy is placed on the core of one of the partials, the edge dislocation climbs up one atomic plane. In this case, the second dislocation can not restore order at the point of vacancy, thus creating a disordered "tube" that exerts a drag on the dislocation. Vacancy hardening can arise if vacancy formation has a lower activation enthalpy, $E_f$, than vacancy migration, $E_m$. That means, at intermediate temperatures vacancies are easily formed but can not readily move. As the vacancy concentration increases with increasing temperature, so does the yield strength. At high enough temperatures, the vacancies begin to migrate thus leading to dislocation creep and a fall in the yield strength. Based on this mechanism, the temperature dependency of the yield strength is represented by a linear fall (with respect to absolute temperature) in region I, an exponential rise superimposed on a linear fall in region II, and another fall due to dislocation creep in region III.

Using FeAl single crystals, Yoshimi *et al.* [18] have also reported that the yield strength peak is coincident with a slip transition from $\langle 111\rangle$ direction at intermediate temperature to $\langle 100\rangle$ at high temperature. They further noted that climb dissociation of $\langle 111\rangle$-type superdislocations occurred within the temperature range of the strength anomaly. Based on these observations, Yoshimi *et al.* also believed that the anomaly is caused by a diffusion-assisted process such as climb dissociation and/or APB dragging.

The FeCo-V material used in our studies has a fine-grained polycrystalline microstructure. This may account for its milder strength anomaly compared with the single crystalline FeAl alloys reported in the literature. The Fe-27Co alloy does not show strengthening at intermediate temperatures but a plateau between regions I and III. It should be pointed out that the composition of this alloy lies just outside the ordered region of the phase diagram.

It was stated earlier that the strength of Fe-49Co-V is rather insensitive to the strain rate in Region II of strength-temperature curve shown in Fig. 6. Close comparison of data in region II reveals an anomalous behavior in that the yield strength is actually even slightly lower at the higher strain rate. This negative strain rate sensitivity is another characteristic of dynamic strain aging. Xiao *et al.* [19] discovered the same phenomenon when they studied the dynamic strain aging in f.c.c. alpha brass. They explained that when the strain rate is higher, shorter time is available for solute clouds to form around the dislocations so the clouds are smaller and dislocations need less stress to move. On the other hand, a higher strain rate makes the dislocations glide faster to the next barrier in the lattice, thus raising the strength. These two opposite forces will lead to the strain-rate insensitivity or negative strain-rate sensitivity of the yield strength. Another observation supporting the dynamic strain aging theory is the appearance of serration in the stress-strain curves of both, Fe-27Co and Fe-49Co-2V, alloys above the room temperature. The serration is more noticeable at the higher strain rate. The amplitude of the serration increases with increasing temperature. The serration disappears above 600 °C in Fe-27Co and above 700 °C in FE-49Co-2V. The occurrence of serration thus appears to coincide with the temperature range of the yield strength anomaly. Similar phenomenon has also been reported for single crystalline [18] and polycrystalline [19] FeAl. It is known that one of the prominent manifestations of dynamic strain aging (DSA) is a serrated yielding region. Some researchers, e.g., Yoshimi *et al.* [16], however, disagree that the observed serration is caused by dynamic strain aging.

## 3.2. The effect of order/disorder

The degree of long-range order was varied in Fe-49Co-2V specimens from an almost fully ordered to a largely disordered state by changing the cooling rate as described earlier. Fig. 7 shows the stress-strain curves from tensile tests conducted at room temperature. The results indicate an increase in the yield strength, but a decrease in the discontinuous yield strain, with decreasing degree of order. Table II gives the values of the yield strength for various cooling rates. It is seen

TABLE II The tensile yield strength of Fe-49Co-2V alloy as a function of the cooling rate from 820 °C

| Cooling Rate | 30 °C/hr | 60 °C/hr | 90 °C/hr | Air cooling | Quenched |
|---|---|---|---|---|---|
| Yield Strength, MPa | 359 | 389 | 385 | 503 | 526 |

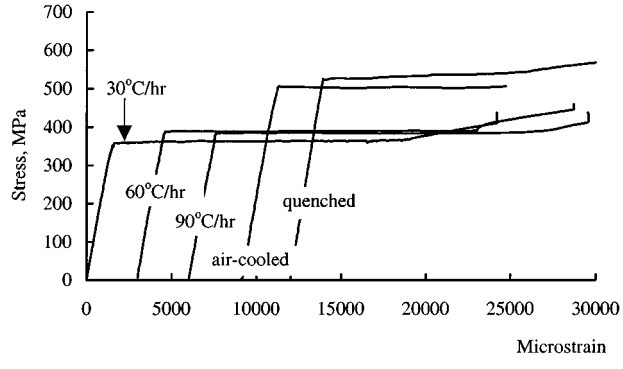


*Figure 7* Tensile stress-strain curves of Fe-49Co-2V alloy showing the effect of long-range order.

that for the three slower cooling rates where the alloy is mostly ordered, the yield strengths are very close to each other and are generally smaller than the yield strengths of the largely disordered specimens, i.e., the air-cooled and brine-quenched test pieces.

Stoloff and Davies [4] studied the order/disorder effect in equimolar FeCo by testing materials with order parameter S ranging from 0 to 0.9. They found that the yield strength exhibited a peak around an intermediate degree of order. They further noted that unlike $Cu_3Au$, ordering had little effect on the strain hardening of FeCo-V alloy. An ordered structure contains superdislocations, which consist of two unit dislocations separated by a strip of APB. The energy of the APB, $E_{OR}$, is dependent on the degree of long-range order, $S$, by $E_{OR} = S^2 E_{OR}^{(s=1)}$, where $E_{OR}^{(s=1)}$ is the energy of the APB corresponding to $S = 1$. So, the lower the long-range order parameter $S$, the lower the energy of APB. At certain low $S$ value, the energy of the APB is so weak that the superdislocations disassociate into their constituent ordinary dislocations, which then can move independently. These gliding unit dislocations will create wrong bonds in their wake thus leading to a hardening similar to that occurring above $T_c$ due to short range order. On the other hand, when $S$ is increased, unit dislocations tend to associate into pairs, namely superdislocations, which glide in an ordered matrix without creating a trail of wrong bonds. The yield strength thus decreases as the proportion of superdislocations increases. Above the transition temperature, the long-range order parameter abruptly drops to 0 and the yield strength is then controlled by short-range order. The higher the short-range order parameter, the higher the yield strength. The short-range order parameter has its maximum at transition temperature where the peak in the yield strength is observed.

Figs 8 to 10 depict SEM images of the fracture surfaces corresponding to the cooling rates of 60 °C/hr, air cooling and brine quenching, respectively. It is seen that fracture becomes more and more ductile with increasing cooling rate; the clearly ductile nature of fracture in the brine quenched specimen is evident from the typical outer shear lips and inner dimpled region (Fig. 10). Fig. 11 shows the dimpled region at a higher magnification.

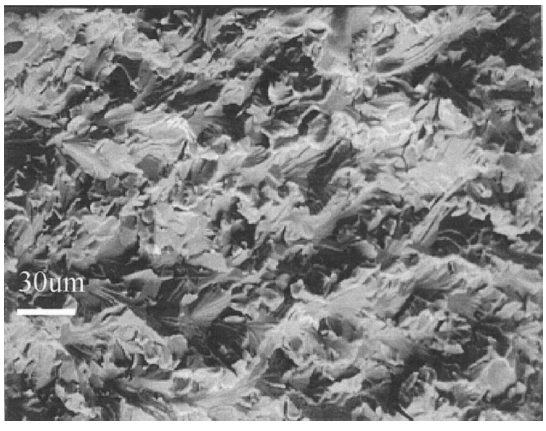


*Figure 8* Fracture surface of Fe-49Co-2V alloy cooled at 60 °C/hr from 820 °C.


*Figure 9* Fracture surface of Fe-49Co-2V alloy air-cooled from 820 °C.

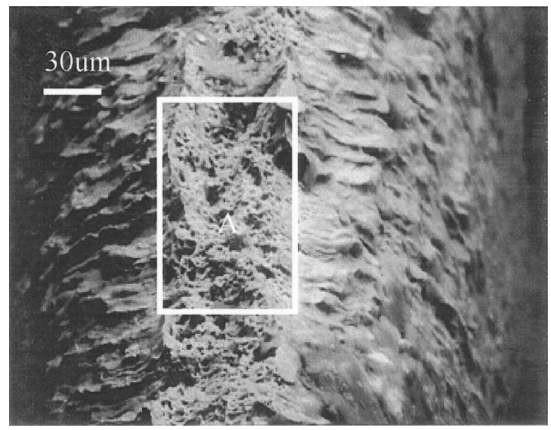


*Figure 10* Fracture surface of Fe-49Co-2V alloy brine-quenched from 820 °C.

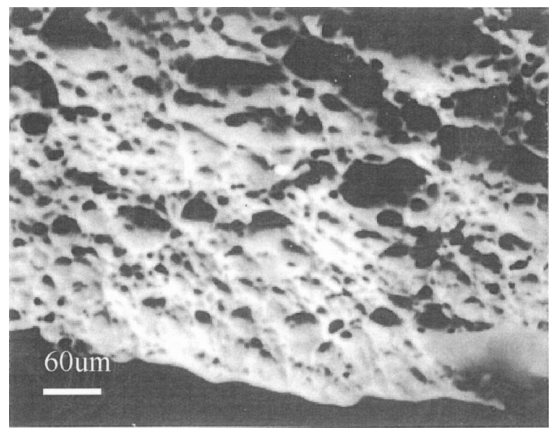


*Figure 11* High-magnification image of area A in Figure 2.10.

## 3.3. The effect of the grain size

The effect of the grain size was studied by annealing both alloys at 820 °C for various duration of time. A longer annealing time corresponds to a larger grain size as shown in Figs 12 and 13 for Fe-27Co and Fe-49Co-2V alloys, respectively. Yu *et al.* [21] have previously reported the kinetics of grain growth in these alloys.

Figs 14 and 15 depict the stress vs. strain curves for Fe-27Co and Fe-49Co-2V samples, respectively, with annealing time ranging from 10 minutes to 20 hours. As the grain size increases, several trends are noted: the

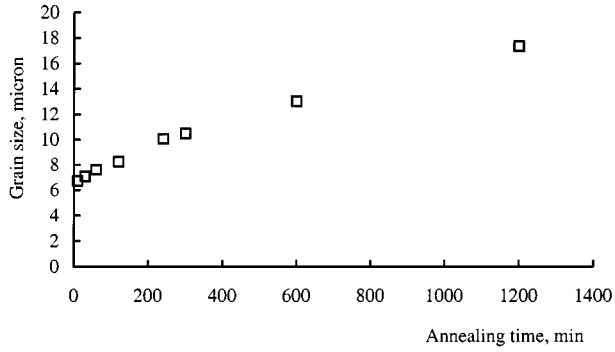


*Figure 12* The variation of the grain size with annealing time for Fe-27Co alloy.

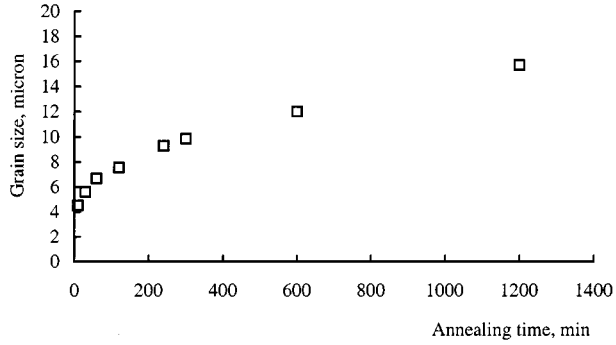


*Figure 13* The variation of the grain size with annealing time for Fe-49Co-2V alloy.

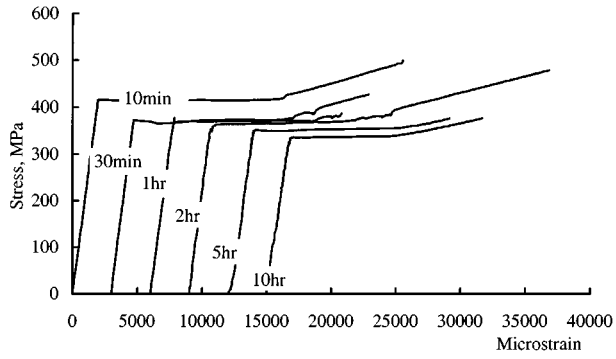


*Figure 14* Tensile stress-grain curves of Fe-27Co alloy as a function of the annealing time at 820 °C to vary the grain size.

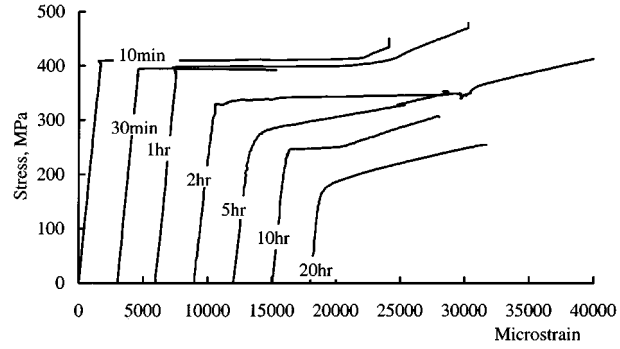


*Figure 15* Tensile stress-grain curves of Fe-49Co-2V alloy as a function of the annealing time at 820 °C to vary the grain size.

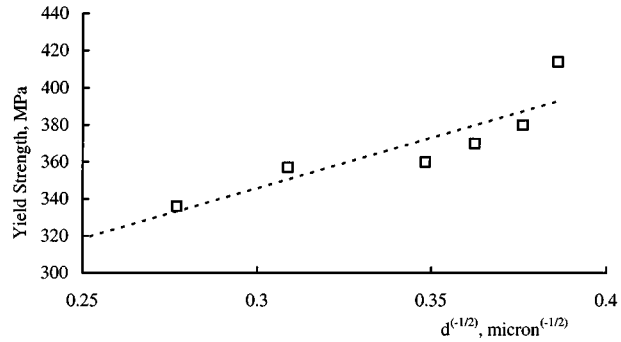


*Figure 16* The effect of grain size on the yield strength of Fe-27Co alloy.

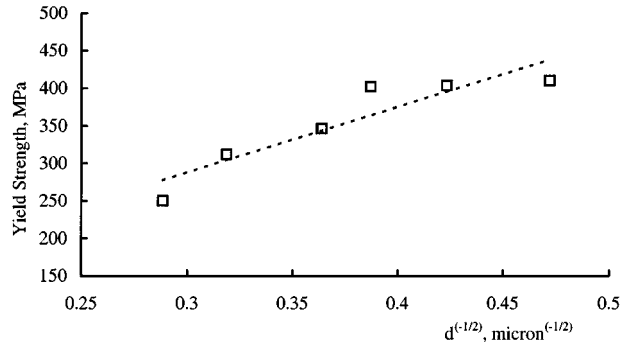


*Figure 17* The effect of grain size on the yield strength of Fe-49Co-2V alloy.

discontinuous yield phenomenon diminishes, the yield strength drops, and the materials becomes less ductile.

Figs 16 and 17 show the variation of the yield stress with grain size for Fe-27Co and Fe-49Co-2V alloys, respectively. The data are fitted to a Hall-Petch type formula where $\sigma_{ys} = \sigma_o + kd^{-1/2}$. The following relationships between the yield stress and grain size are obtained:

$$\sigma_{YS} = 164.03 + 615.27d^{-1/2} \quad \text{for} \quad \text{Fe-27Co}, \qquad (1)$$

and

$$\sigma_{YS} = 25.57 + 847.59d^{-1/2} \quad \text{for} \quad \text{Fe-49Co-2V}. \qquad (2)$$

Table III compares the values of $k$, $\sigma_o$, and $\theta$ (at 1% strain) along with the results obtained by other researchers for various Fe-Co compositions [7, 22]. For Fe-49Co-2V, the $k$ and $\theta$ measured in this investigation are reasonably close to those reported by Zhao and Baker [7], however, $\sigma_o$ is significantly smaller than the values obtained by Zhao and Baker [7] or by Jordan and Stollof [22]. Zhao and Baker proposed the following relationship between the discontinuous yielding strain and grain size: $\varepsilon_L = k/\theta\, d^{-1/2}$. Here, $\varepsilon_L$ is the discontinuous yielding strain, $k$ is the Hall-Petch parameter, $\theta$ is the work-hardening rate, and $d$ is the grain size. For Fe-27Co, it is found that $\theta$ decreases from 8.1 GPa to 5.8 GPa when annealing time is increased from 10 min to 10 hrs. For Fe-49Co-2V, $\theta$ varies from 12 GPa to 7.4 GPa within the same range of annealing times. Using the above relationship it is found that calculated values of $\varepsilon_L$ are consistently about twice the measured values. It can therefore be assumed that $\varepsilon_L \propto k/\theta \cdot d^{-1/2}$.

TABLE III Values of $k$, $\sigma_o$ and work-hardening rate, $\theta$ for FeCo alloys O represents ordered and D represents disordered states

| Composition | Fe-49Co-2V (This research) | | Fe-27Co (This research) | | Fe-30Co [17] | | Fe-50Co [17] | | Fe-49Co-2V From [19] | |
|---|---|---|---|---|---|---|---|---|---|---|
| State | O | D | O | D | O | D | O | D | O | D |
| K(MPa$\mu$m$^{1/2}$) | 847 | — | 615 | — | 724 | 141 | 806 | 456 | 660 | 220 |
| $\sigma_o$ (MPa) | 26 | — | 164 | — | 149 | 237 | 172 | 309 | 150 | 360 |
| $\theta$ at 1% strain (GPa) | 7.4 ~ 12 | — | 5.8 ~ 8.1 | — | 7.7 | 5.8 | 7.6 | 6.7 | — | — |

## 4. Conclusion

The effects of temperature, grain size, and order/disorder on the tensile behavior of Fe-27Co and Fe-49Co-2V alloys were studied. The Fe-49Co-2V undergoes an order/disorder transformation at a temperature of 725 °C. The ordered alloy has a B2 structure similar to the well-studied FeAl. The temperature dependence of the yield strength of Fe-49Co-2V closely resembles that of FeAl in that an anomalous strengthening is observed in the temperature range 300 °C to 700 °C. A peak in the yield strength appears at around 700 °C (approx. 0.45 $T_m$). The yield strength is insensitive to strain rate within the temperature range of the anomalous behavior. Possible mechanisms for this anomaly have been discussed. Both alloys show discontinuous yielding at lower temperature and serration in the stress-strain behavior within the temperature range of the strength anomaly.

Long-range order leads to a decrease in the yield strength of Fe-49Co-2V alloy; the ordered alloy exhibits a larger discontinuous yielding strain.

The yield strength vs. grain size of both alloys follows a hall-petch type relationship where $\sigma_{ys} = \sigma_o + kd^{-1/2}$. Also for both alloys, the discontinuous yielding strain obtained at room temperature is proportional to $k/\theta \cdot d^{-1/2}$ where $\theta$ is the strain hardening coefficient. The magnitude of $\theta$ depends on the grain size and decreases with increasing grain size.


## Acknowledgement

This investigation was conducted with support from the Air Force Office of Scientific Research under the AFOSR F49620-96-1-0434.


## References


1. N. S. STOLOFF, R. G. DAVIES and R. C. KU, *Transactions of the Metallurgical Society of AIME* **233** (1965) 1500.
2. N. S. STOLOFF and R. G. DAVIES, *Acta Metallurgica* **12** (1964) 473.
3. C. W. CHEN, *J. Appl. Phys.* **32**(3) (suppl.) (1961) 348.
4. Y. G. KOYLU, G. F. HANCOCK and R. D. RAWLINGS, *Phy. Stat. Sol.* (a) **16** (1973) 73.
5. C. D. PITT and R. D. RAWLINGS, *Metal Science* **17** (1983) 261.
6. L. ZHAO, I. BAKER and E. P. GEORGE, *MRS Symp. Proc.* **288** (1993) 501.
7. L. ZHAO and I. BAKER, *Acta Metall. Mater.* **42**(6) (1994) 1953.
8. R. G. DAVIES and N. S. STOLOFF, *Transactions of the Metallurgical Society of AIME* **236** (1966) 1605.
9. G. W. ARDLEY and A. H. COTTRELL, *Proc. Royal. Soc.* **219** (1953) 328.
10. A. LAWLEY, E. A. VIDOZ and R. W. CAHN, *Acta Metall.* **9** (1961) 287.
11. Y. UMAKOSHI, M. YAMAGUCHI, Y. NAMBA and K. MURAKAMI, *ibid.* **24** (1976) 89.
12. A. NOHARA, M. IZUMI, H. SAKA and T. IMURA, *Phys. Stat. Sol.* (a) **82** (1984) 163.
13. D. CAILLARD, *MRS Symp. Proc.* **364** (1995) 17.
14. I. BAKER and D. J. GAYDOSH, *Mater. Sci. Eng.* **96** (1987) 147.
15. H. XIAO and I. BAKER, *Scripta Metall. Mater.* **28** (1993) 1411.
16. D. G. MORRIS, *Phil. Mag.* **71** (1995) 1281.
17. I. BAKER and E. P. GEORGE, *MRS Proc.* **460** (1997) 373.
18. K. YOSHIMI, S. HANADA and M. H. YOO, *MRS Proc.* **460** (1997) 313.
19. L. G. XIAO, *Scripta Metall.* **22** (1988) 179.
20. D. G. MORRIS, J. C. JOYCE and M. LEBOEUF, *Phil. Mag. A* **69** (1994) 961.
21. R. H. YU, S. BASU, Y. ZHANG, A. PARVIZI-MAJIDI and J. Q. XIAO, *J. Appl. Phys.* **85** (1999) 6655.
22. K. R. JORDAN and N. S. STOLOFF, *Transactions of the Metallurgical Society of AIME* **245** (1969) 2027.



*Received 6 October 1999*
*and accepted 14 August 2000*